




Mapping the Palaeo-Piniada Valley, Central Greece, Based on Systematic Microtremor Analyses

A. MANTOVANI,^{1,2} S. VALKANIS,³ D. RAPTIS,⁴ and R. CAPUTO^{1,2,5} 

Abstract—The application of seismic noise-based techniques has become particularly popular in the last decades, as they are not invasive and do not require large teams or expensive equipments. The Horizontal to Vertical Spectral Ratio (HVSr) is commonly used not only in seismic microzoning studies as far as from noise recording constraining the fundamental resonant frequency, but it is also possible to infer the depth of the bedrock knowing the average shear wave velocity of the overlying sedimentary cover, or viceversa (i.e. resonance equation). For the purposes of the present research, more than 300 single-station noise measurements were carried out across the Piniada Valley (Central Greece), along and between several transects planned roughly perpendicular to the mean valley trend. To understand the palaeogeographic and tectonic evolution of this area, we needed an estimation of the geometry at depth of the bedrock underlying the fluvial deposits of the present-day Pinios River. As a result, for each measured site, we calculated the depth of the bedrock and, afterwards, such values were opportunely interpolated for obtaining a 3D model of the palaeo-Piniada Valley documenting for the first time the recent (Late Quaternary) inversion of the topographic gradient.

Key words: Seismic noise, HVSr, mapping, Thessaly, geophysical survey.

1. Introduction

Alluvial plains are generally the locus of fluvial deposition, whose accumulation rate depends on several factors, such as the creation of

accommodation space generally by tectonic activity, the dimension of the upstream hydrographic basin, the regional climate conditions and the water discharge and its seasonal regimes, the outcropping lithologies in the catchment area and hence the amount of bed and suspended load and their proportion, the mean gradient of the plain as well as of the main water course, the occurrence and/or formation of local base levels and/or knick points and their relative altitude. When alluvial plains develop in intermountain conditions, the overall geometry of the sedimentary bodies infilling the lower part of the valley is obviously not tabular but characterized by a lense shape in section view with a roughly flat top surface and a more or less concave lower surface.

The longest river draining Greece is represented by the Pinios (216 km) that collects waters from large sectors of the Antichasia, Pindos and Othris mountains as well as the western Pilion and southern Olympus, with a total extension of ca. 9500 km² (Fig. 1). If we consider the whole drainage pattern, the existence of some major hydrographic anomalies could be observed (e.g. Migiros et al. 2011) and particularly the occurrence of subsequent reaches alternatively flowing across wide alluvial plains, like the Karditsa Plain to the west and the Larissa Plain to the east, narrow valleys like the Piniada and the Gonnoi ones, and even three gorges (Kalamaki, Rodia and Tembi; Fig. 1).

It is noteworthy that the general gradient of the numerous affluents that progressively merge downstream from Antichasia, Pindos and Othris rapidly decreases once the water courses get into the Karditsa Plain. Indeed, they commonly enter the plain at about 130–150 m altitude, while the Pinios River exits the plain near Farkadona at ca. 90 m a.s.l. (Fig. 2), from

Electronic supplementary material The online version of this article (<https://doi.org/10.1007/s00024-017-1731-7>) contains supplementary material, which is available to authorized users.

¹ Department of Physics and Earth Sciences, University of Ferrara, Ferrara, Italy. E-mail: rcaputo@unife.it

² Centro interuniversitario per la ricerca sismotettonica, CRUST-UniFE, Ferrara, Italy.

³ Koronidos str., 9, 42131 Trikala, Greece.

⁴ New Energies And environment - NEA S.r.l., Ferrara, Italy.

⁵ Research and Teaching Center for Earthquake Geology, Tyrnavos, Greece.

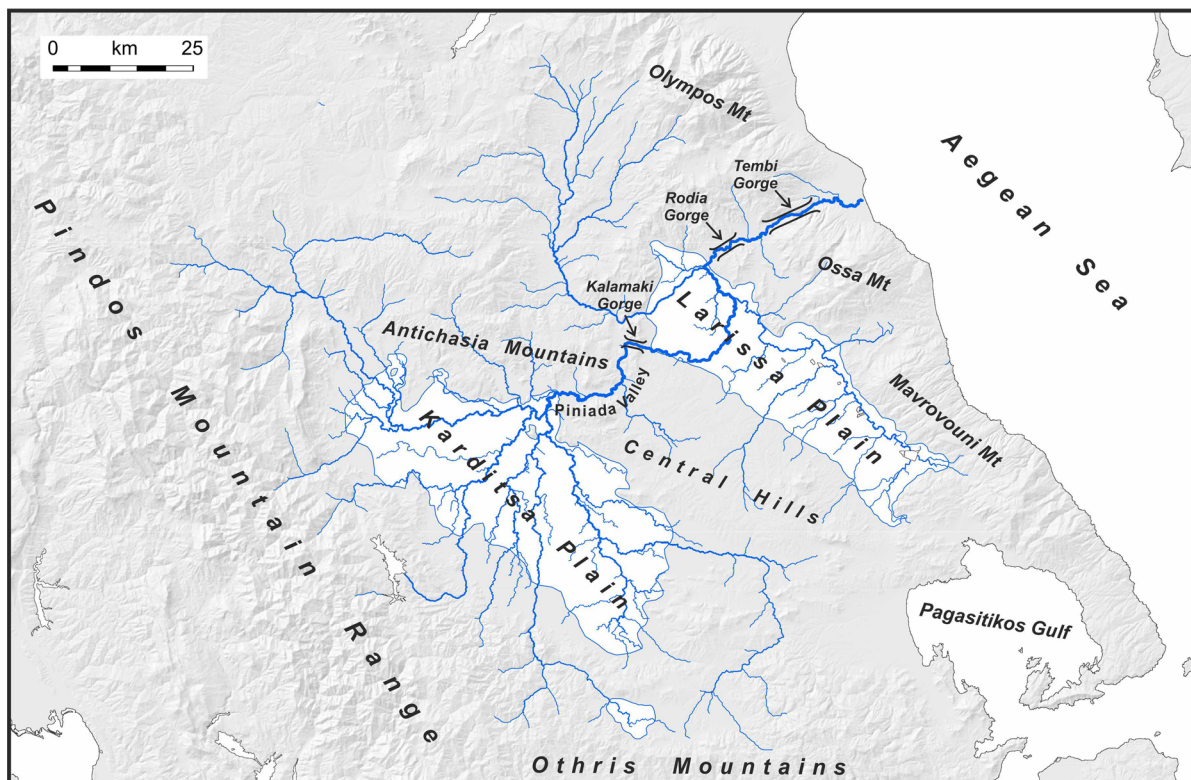


Figure 1

Hydrographic network of the Pinios River draining large sectors of Central Greece and location of the Piniada Valley, investigated in the present research, separating the western Karditsa Plain from the eastern Larissa Plain

where it still has to flow for ca. 150 km before reaching the delta and hence the final base level of the Aegean Sea.

In the present paper, we focus on the hydrographic anomaly characterizing the reaches between the two major plains, Karditsa and Larissa, west and east, respectively, and particularly where the Pinios River flows across the Piniada Valley and the Kalamaki Gorge. The former morphological feature is characterized by a 1–3-km-wide alluvial plain bordered by the Palaeozoic–Triassic bedrock belonging to the Pelagonian Zone (Fig. 2; IGME 1985, 1998; Caputo 1990; Doutsos et al. 1993). This intermountain valley bottom progressively narrows downstream to few hundred metres north of the village Koutsochero and completely disappears in correspondence of the Kalamaki Gorge, where the river bed is directly entrenched in the sloping bedrock. In the former reach, the river is characterized by several meanders

with a sinuosity index (the ratio between the length of a river bed measured from two sections and their linear distance) of ca. 1.6, while in the final sector and especially within the gorge the river geometry is almost linear and sinuosity drops to ca. 1. Due to the reduced width of the Piniada Valley and the paucity of permanent agricultural crops, no major land reclamation works took place in this sector of Pinios River, allowing the river meanders to evolve and migrate naturally up to this date.

These morphological and hydrological premises embody the main question posed in this paper. Indeed, the major aim of this research is to reconstruct the geometry at depth of the Piniada Valley and particularly of the bedrock underlying the fluvial deposits that have been aggraded during Late Quaternary, partially infilling the intermountain valley. To achieve this goal, we systematically investigated the area and carried out more than 300 single-station

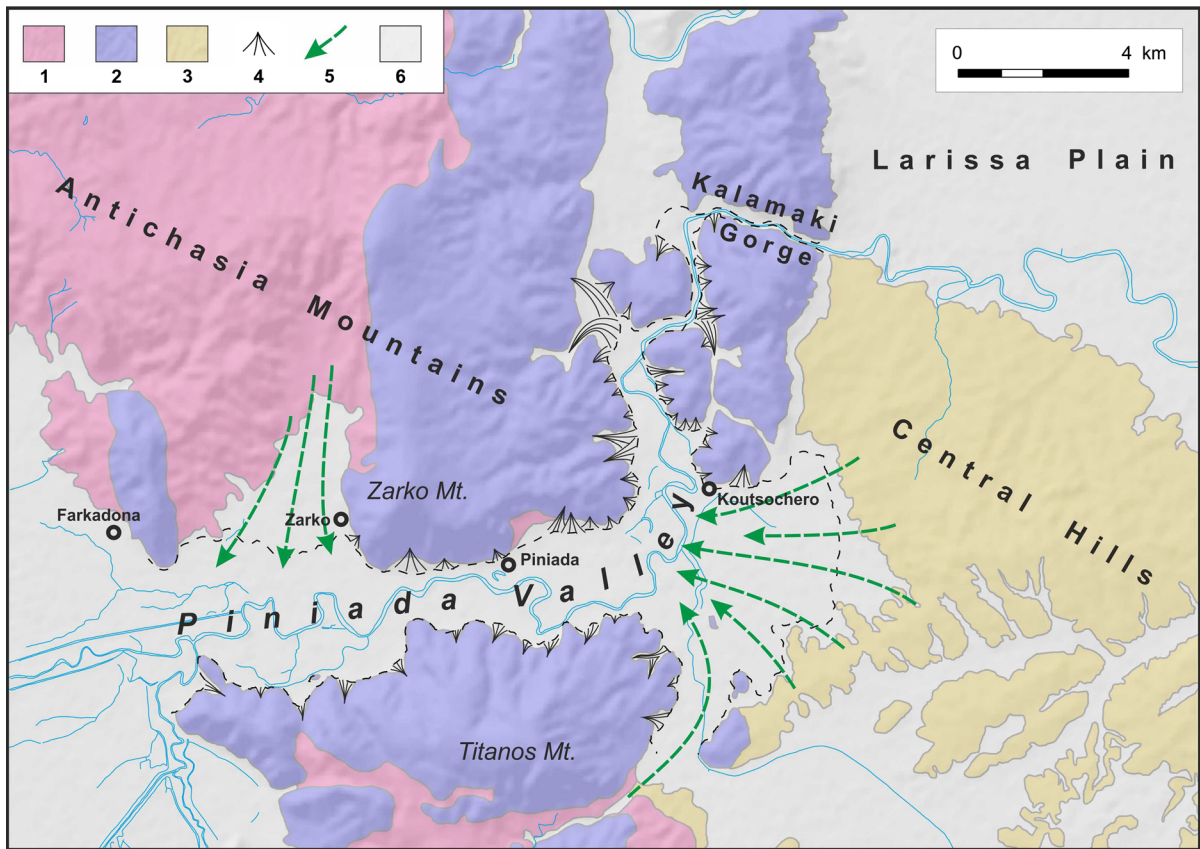


Figure 2

Simplified geological map of the investigated area. 1 Palaeozoic gneiss and schists; 2 Triassic–Lower Jurassic recrystallized limestones; 3 Pliocene–Early Pleistocene fluvio-lacustrine deposits; 4 Late Pleistocene ejection cones (from carbonate rocks); 5 Late Pleistocene ejection cones (from Palaeozoic and Neogene–Quaternary rocks); 6 Holocene alluvial deposits. The black dashed line borders the present-day fluvial plain of the Pinios River. Green arrows indicate the transport paths of the fine-grained clastic material eroded from the Central Hills and the Antichasia Mountains. See text for discussion on their role in varying the shear-wave velocity of the Piniada Valley infilling

seismic noise measurements that allowed to map the lateral variations of the natural frequency within the fluvial plain. Based on the available stratigraphic logs in correspondence of some deep boreholes for irrigation purpose, we could also calibrate the peaks observed in the corresponding HVSR curves and hence constrain the depth of the major impedance contrast (i.e. the seismic bedrock).

The investigation strategy was, first, to produce several pseudo-2D transects based on high-density aligned measurements across the valley and subsequently to cover the entire area with a less dense, but relatively regular, grid of measured sites. All depth-converted measurements were then properly interpolated for obtaining a 3D model thus reconstructing

the geometry of the seismic bedrock along the Piniada Valley. We anticipate here the major result of this research that clearly documents the presence at depth of a palaeovalley sloping in the opposite direction of the present-day river flow.

2. Methodology

The background noise, also referred to as micro-tremor, is present everywhere at the Earth's surface and its sources, and thus its frequency content, are related to both atmospheric phenomena and anthropogenic activities (Gutenberg 1958; Asten 1978; Asten and Henstridge 1984). It is generally

characterized by very small oscillations (10^{-4} to 10^{-2} mm) with spectral components poorly attenuated in space and measurable with passive recording techniques. All elastic waves during their path from the source to a site suffer some attenuation which is basically geometric, due to the increasing dimensions of the wave front, and anelastic (or intrinsic), due to the real not perfectly elastic behaviour of all rocks and especially sediments. In all cases, the amount of attenuation is a function of frequency; indeed, assuming a constant velocity for all frequencies, the shorter the wavelength (i.e. the higher the frequency) the greater the number of cycles and hence the intrinsic attenuation that occurs. Accordingly, stratigraphic layering governs the distribution of the mechanical and geophysical properties; therefore, such information is included in the recorded microtremors together with random noise (e.g. Castellaro et al. 2005). Information on the subsoil can be deduced by means of several geophysical methods like that proposed by Nakamura (1989) with his horizontal to vertical spectral ratio (HVSr). This technique is nowadays largely used to estimate the principal resonance frequencies of the subsoil, while a general consensus about the capability of this technique to provide a reliable estimation of the local seismic amplification has not been reached so far (e.g. Nakamura 1989, 2000; Lermo and Chavez-Garcia 1993; Bard 1998; Mucciarelli and Gallipoli 2001 and references therein; SESAME European project 2005). Notwithstanding, such outcomes represent crucial information for microzoning studies, for mapping subsoil interfaces and also for engineering antiseismic planning (e.g. Ibs-von and Wohlenberg 1999; Mucciarelli and Gallipoli 2001; Parolai et al. 2001; Gallipoli et al. 2004; Hinzen et al. 2004; D'Amico et al. 2008; Gosar and Lenart 2010; Mundepi and Mahajan 2010; Albarello et al. 2011; Matsushima et al. 2014; Paolucci et al. 2015; Mantovani 2016; Tarabusi and Caputo 2016).

Even if the theoretical basis of the H/V still remains a matter of debate, the outcome is an experimental curve representing the ratio between the mean spectral amplitude of microtremors (horizontal to vertical components) as a function of frequency. The H/V curve exhibits peaks linked to the resonance frequencies of the soil beneath the measured site.

Therefore, as already mentioned, this method highlights the occurrence of resonance phenomena and provides an estimation of the frequencies at which the ground motion can be amplified, as a result of site effects induced by the presence of stratigraphic discontinuities, and thus modifications in the geophysical properties within the subsoil.

In case of a single-layer one-dimensional stratigraphy overlying a highly contrasted infinite bedrock (Lermo and Chavez-Garcia 1993, 1994; Lachet and Bard 1994; Ibs-von and Wohlenberg 1999; Fäh et al. 2001), the principal S-wave resonance frequency of the sedimentary cover, f_0 , also referred to as fundamental resonance frequency, is linked to its average shear wave velocity, v_s , and thickness, h , according to the following formula (i.e. the so-called resonance equation):

$$f_0 = \frac{v_s}{4 \cdot h} \quad (1)$$

Therefore, once f_0 is constrained, the H/V technique can provide stratigraphic information as it is possible to obtain the thickness of the sedimentary cover knowing its average shear wave velocity, or viceversa.

In case of multilayer subsoil system, more complex approaches and hence modelling strategies would be preferable (Tsai and Housner 1970; Ben-Menahem and Singh 1981; Aki and Richards 2002; Scherbaum et al. 2003; Ohrnberger et al. 2004; Oliveto et al. 2004; Castellaro and Mulargia 2009; Lunedei and Albarello 2010, 2015; Sánchez-Sesma et al. 2011; Lontsi et al. 2015; Kawase et al. 2015). This led in the last years to the implementation of different computation methods in dedicated software for the elaboration and/or inversion of the H/V curves, as for example Grilla (<http://www.moho.world>), Geopsy (<http://www.geopsy.org>), ModelHVSr (Herak 2008) and OpenHVSr (Bignardi et al. 2016). However, the geological setting of our investigated area satisfies, at a first approximation, the single-layer stratigraphic model with high impedance contrast, therefore, allowing us to simply and directly apply Eq. (1) without any other, more sophisticated, inversion procedures.

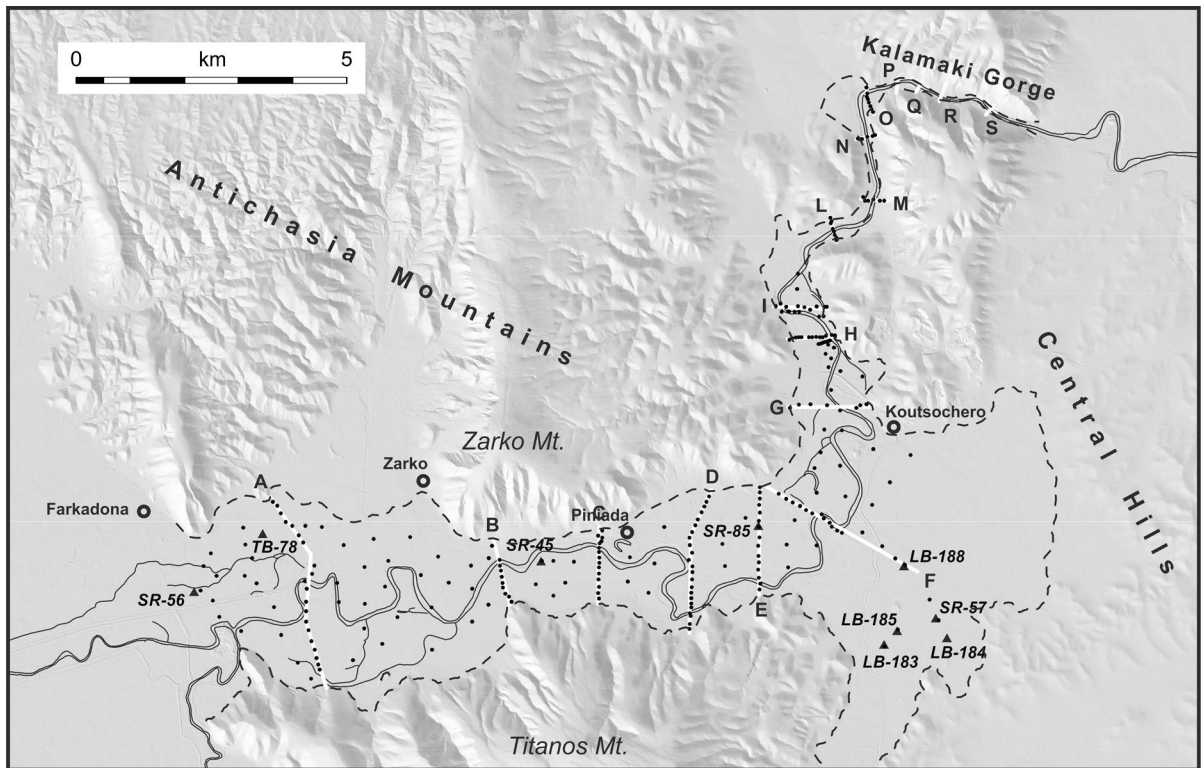


Figure 3

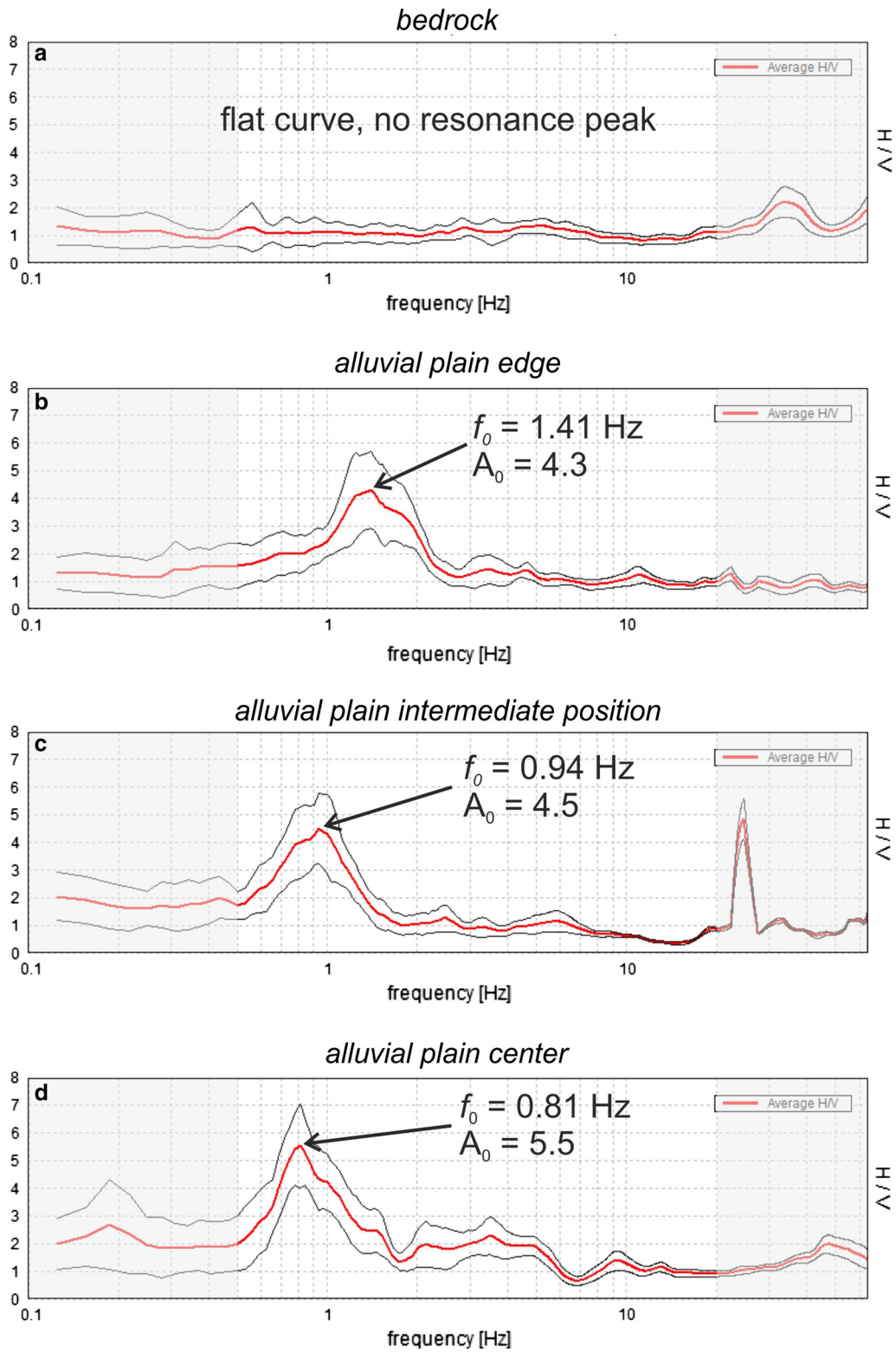
Shaded relief map showing the location of the HVSR measurements within the Piniada Valley (black dots) and the traces of the pseudo-2D sections (white segments) reconstructed in the first working phase. Capital letters label the traces. The boreholes used for constraining the shear-wave velocity of the sediments infilling the valley are also represented (triangles). The path of the modern Pinios River (thin double line) and the boundaries of the fluvial plain (dashed line) are also shown for reference

3. Data Acquisition and Analyses

An extensive geophysical survey based on more than 300 single-station noise recordings was performed all over the Piniada Valley (Central Greece; Fig. 3). The measurements have been carried out using a digital tomograph, Tromino^(R) (<http://www.moho.world>), an all-in-one instrument with a three-component short-period seismometer (proper frequency equal to 4.5 Hz) expressly designed for noise measurements and maximum portability, already used by several teams of researchers for detecting frequencies even lower than 1 Hz (Castellaro et al. 2005; D'Amico et al. 2008; Herak et al. 2010; Albarello et al. 2011; Chatelain and Guillier 2013; Paolucci et al. 2015; Mulargia and Castellaro 2016, among many others).

As suggested by the SESAME guidelines (Koller et al. 2004; Bard et al. 2005; SESAME European project 2005), to ensure a good in situ soil–sensor coupling and to prevent low-frequency disturbances, the instrument was placed in a small and flat pit purposely prepared and well coupled with the ground, the measurements were carried out during favourable meteorological conditions and not close to buildings and/or tall trees. During the geophysical campaigns, at selected sites a second measurement has been performed at different times for checking repeatability of the results and in all cases the comparison of the outcomes confirm the stability of the fundamental resonance frequency and, therefore, the reliability of the results.

At each measuring site, noise signal was recorded at 128 Hz sampling rate for recording times lasting between 30 and 18 min and subsequently analysed



◀Figure 4

Examples of HVSr curves obtained using the Grilla software emphasizing the local natural frequency and its amplitude. The examples have been selected from different settings, like **a** bedrock sites close to the border of the plain (PV005), **b** at the valley edge within the plain (PV136), **c** at an intermediate distance (PV144) from **d** the middle of the alluvial plain (PV167). The natural frequencies and amplitudes calculated for all sites are listed in the Supplementary material

using the Grilla software provided by MoHo (<http://www.moho.world>). The HVSr analysis is performed, first, by subdividing the acquired signal for each component into non-overlapping time windows of 30 s. Each window was detrended, tapered with a Bartlett window and padded with zeros. The Fast Fourier Transform (FFT), as well as the amplitude spectrum, was subsequently computed for each window. The spectra were smoothed according to a triangular smoothing function with a width equal to 10% the central frequency. The HVSr ratio (i.e. the geometric average of the horizontal components over the vertical one) was calculated for each frequency and the spectral ratios of each time window were then averaged. Finally, the mean HVSr curve was computed along with the 95% confidence interval.

In some cases, the HVSr curves exhibit spurious peaks as a result of localized anthropogenic sources (e.g. water pumps, road traffic, industrial activities). In line with the SESAME recommendations (SESAME European project 2005; Koller et al. 2004; Bard et al. 2005), such transients should be removed, especially if their frequencies are comparable to those under investigation. Therefore, we proceeded by analysing both the time stability of spectral ratios and their directionality (i.e. projection of the HVSr along different directions, from 0° to 180°) in 10° angular intervals. When strong transients occur, the corresponding temporal window is identified and neglected from further computation. Accordingly, as above explained, the mean HVSr curve represents the average of such ratio in each considered time window.

Although a broader range of frequencies could be safely investigated by this approach, we limited our analyses between 0.1 and 64 Hz, while only maxima

inside the frequency range 0.5–20 Hz were taken into account for the subsequent interpretation.

Moreover, before interpreting the HVSr curves we verified the international criteria for ‘stability’ of results (SESAME European project 2005). The first requirement concerns the reliability of the HVSr curve (i.e. significant cycles and sufficient number of windows for a given frequency f_0 , and acceptably low level of scattering between all windows) and the second regards the clarity of the HVSr peak (i.e. fulfilment of amplitude and stability of the peak).

In Fig. 4 are thus represented four examples of HVSr curves, including their 2σ uncertainties, selected from our dataset to represent different geological settings, like bedrock sites close to the border of the plain (a), sites at the valley edge but within the alluvial plain (b), at an intermediate distance (c) and at a middle point of the plain (d). In the Supplementary material the complete set of analyses (S1 to S4) performed for the four selected sites is also reported to show the whole procedure followed in this research.

The above-described analytical process has been applied to all measured sites and both natural frequencies and amplitudes obtained and used in this work are included in the Supplementary material.

Within a narrow intermountain valley flanked by rocky slopes and partially infilled by Late Quaternary loose or poorly condensed fluvial deposits, it is reasonable to expect a high-density contrast and hence an abrupt seismic velocity change in correspondence of the interface separating the Late Quaternary terrigenous deposits and the underlying carbonate and metamorphic rocks (Late Palaeozoic–Mesozoic). Accordingly, these geomechanical conditions are favourable to be detected on the basis of the Nakamura (1989) technique and indeed, most of our HVSr curves are characterized by a clear and often sharp peak locally reaching an amplification factor greater than 10.

As previously mentioned, our research strategy has foreseen two major phases: first, we carried out the measurements at shortly spaced sites (100–200 m in average) aligned along transects planned roughly perpendicular to the mean valley trend (Fig. 3). We carried out seventeen of such profiles from near Farkadona, downstream to the Kalamaki Gorge,

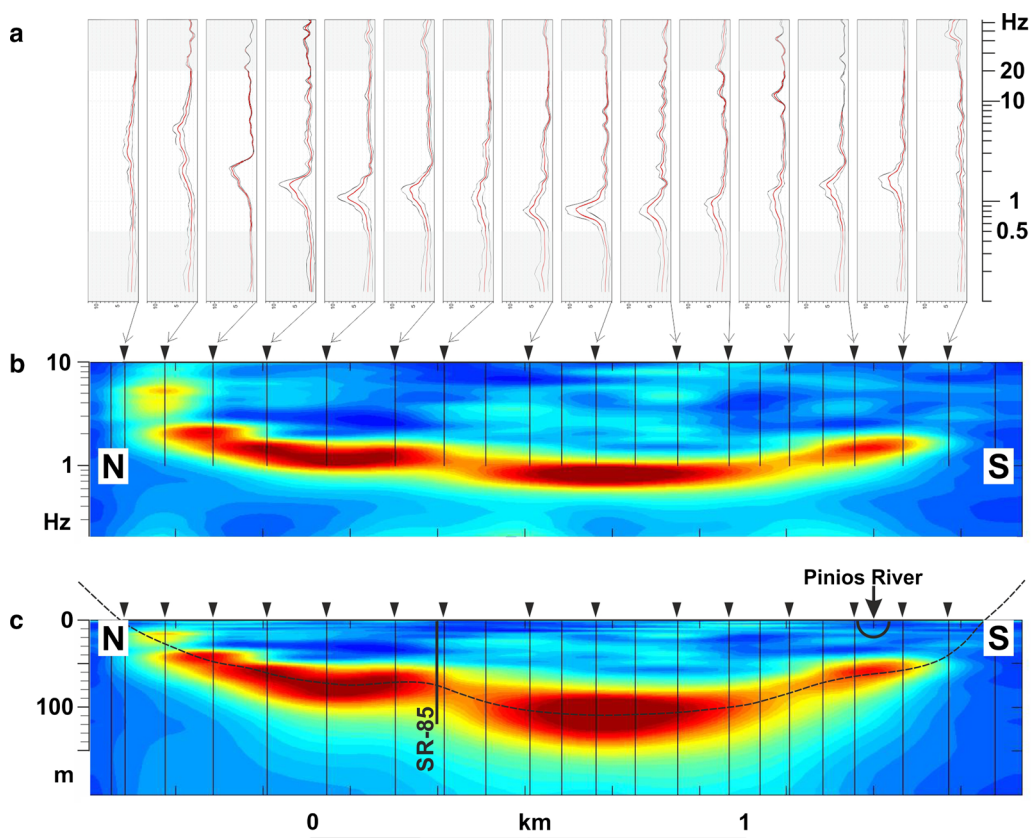


Figure 5

Example of pseudo-2D section reconstructed on the basis of the numerous HVSR measurements. In **a** the HVSR spectra are plotted side-by-side, while in **b** they are interpolated using the Matlab routine developed by Herak et al. (2010) represented in the frequency domain. In **c** is the same profile depth converted based on the shear-wave velocity inferred for this section (see text for discussion). Triangles indicate the projection of the measurement points along the transect (*E* in Fig. 7). The dashed line in figure **c** correlates the depth-converted natural frequency peaks corresponding to the major resonant surface underlying the alluvial plain. This surface likely represents the top of the seismic bedrock, here corresponding to the Triassic limestones or Palaeozoic metamorphic basement. The position of the borehole SR-85 is also reported

respectively, west and east along the Piniada Valley. With the exception of some points located practically at the foot of the bounding slopes for instrumentally verifying the lack of amplification (i.e. bedrock at the zero depth), for each profile all points have virtually the same altitude corresponding to a basically flat topography, which is horizontal in section view. By projecting on the selected profile the HVSR curves of all sites measured within a distance of less than 100 m from the trace and correlating the fundamental frequency peaks, it was possible to reconstruct pseudo-2D sections. To this aim we exploited the Matlab routine “HVSR-profile” proposed by Herak et al. (2010). An example of pseudo-2D section in the frequency domain is represented in Fig. 5b, where the

section is reconstructed as a simple side-by-side stack of observed HVSR spectra (Fig. 5a) taking into account their relative distances along the profile and properly smoothed to tentatively correlate the nearby peaks (Herak et al. 2010).

4. Discussion

4.1. Seismic Bedrock

Based on the geology of the broader area (IGME 1985, 1998; Caputo 1990), the bedrock underlying the Late Quaternary infilling of the Piniada Valley basically corresponds to the Triassic limestone and

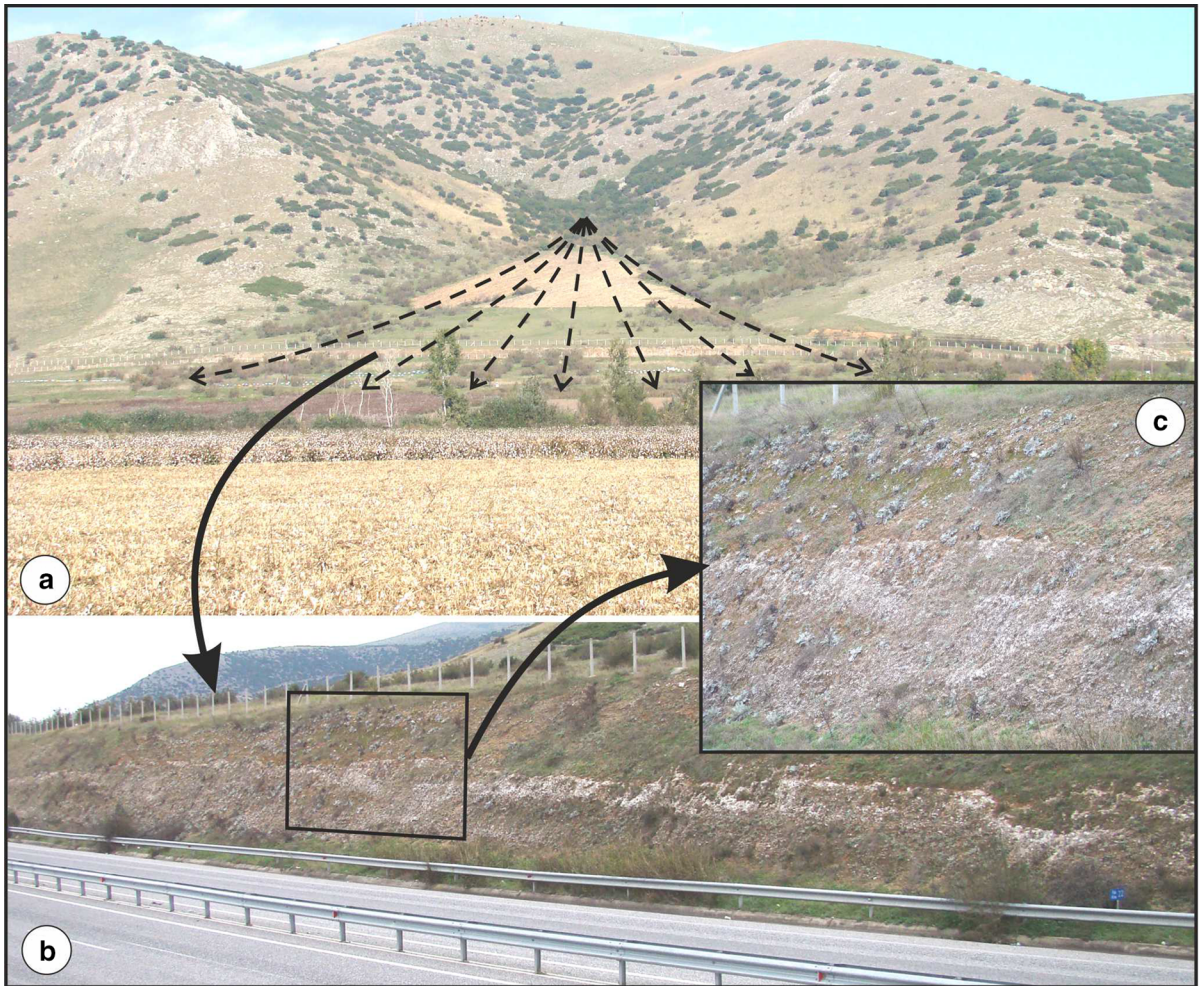


Figure 6

Example of ejection cones characterized by coarse-grained carbonate breccias particularly well cemented especially on their top layers

the Palaeozoic schists–gneiss, both belonging to the Pelagonian Zone and largely outcropping within the investigated area and particularly along the slopes bounding the intermountain valley. As previously described, in the Central Hills east and southeast of Koutsochero village the Pliocene clastic deposits of fluvio-terrestrial origin crop out. In this sector of the plain, which is in any case outside the area investigated with microtremor measurements, these Neogene deposits could be possibly interposed stratigraphically between the Mesozoic rocks and the Upper Pleistocene sediments.

A particular discussion deserves the identification of the bedrock top surface from a seismic point of

view, that is to say, in correspondence of the major impedance contrast occurring in the subsoil of the alluvial plain. As mentioned above, the lateral slopes of the Piniada Valley are affected by erosional phenomena mainly associated with, and consequence of, several minor entrenched valleys. In correspondence of these morphological features typical ejection cones have been formed. Where carbonate rocks (i.e. Triassic limestone) prevail in the hydrographic basin, the cones developed at the base of the minor valleys consist of more or less well-organized carbonate breccias, locally alternating with thin red soils. The breccia layers contain heterometric, but generally coarse, carbonate subangular clasts.

Table 1

List of the boreholes used for the calibration of the HVSR measurements, based on the drilled bedrock depth compared with the natural frequency (f_c) obtained for the site, thus allowing to calculate the average shear-wave velocity (v_s)

Borehole	Bedrock depth (m)	# HVSR measurement	f_c (Hz)	HVSR peak	v_s (m/s)
LB188	103	PV224	0.78	5.4	321
SR85	77	PV166	1.06	3.9	326
LB184	77	PV228	1.10	2.7	339
SR56	155	PV237	0.59	6.3	366
TB78	102	PV243	0.94	5.5	384
SR45	89	PV275	1.09	5.1	388
SR57	90	PV227	1.13	2.7	407
LB185	60	PV229	1.75	4.2	420
LB183	67	PV230	1.63	3.6	437

See Fig. 3 for their location

Especially the upper levels are typically characterized by a diffuse and pervading spatic calcite that makes the whole depositional succession particularly hard in terms of mechanical and seismic behaviour. At this regard, where such cones are exposed, for example along road cuts or quarries, they always appear well cemented and completely lithified (Fig. 6). Some of the microtremor measurements have been purposely carried out in this geological–morphological contest on top of these ejection cones; the lack of any amplification frequency de facto confirms the assumption that these materials could represent the local seismic bedrock within the investigated area. Accordingly, also this lithology shows a high impedance contrast with the overlying loose-to-poorly consolidated alluvial sediments.

4.2. Shear-Wave Velocities

The Matlab routine “HVSR-profile” (Herak et al. 2010) also permits to convert the single curves, and hence the entire profile, from the frequency domain to the depth domain by introducing an average shear-wave velocity of the sediments overlying the impedance contrast surface. At this regard, we spent a particular care in analysing the available stratigraphic logs from boreholes drilled in the 70s within the Piniada Valley for irrigation purposes. In particular, we carried out microtremor measurements in correspondence of these boreholes and compared the obtained HVSR curves for correlating the natural

frequency with the local stratigraphy. The prevailing overlying sediments consist of clay, silt and sand occasionally containing some gravels, always loose or poorly consolidated. The peak observed in the corresponding HVSR curves has been associated with the occurrence of the bedrock, which is commonly represented by the Triassic limestones. In correspondence of the ejection cones descending the minor lateral valleys and buried by the fluvial deposits, the local bedrock is represented by well-cemented conglomerates and breccias as largely observed in outcrops. Based on the depth of the stratigraphically constrained seismic bedrock and the geophysically obtained natural frequency, the average shear-wave velocity of the upper layer has been calculated using Eq. (1) for each borehole. All obtained velocities range between 321 and 437 m/s (Table 1), which are realistic values for the drilled lithologies (Bourbié et al. 1987; Gomberg et al. 2003; Herak et al. 2010; Parker and Hawman 2012).

To exploit this punctual information and for extending it to the whole dataset of more than 300 HVSR measurements, we also took into account the overall geological setting of the area. In particular, we should consider that the sedimentary infilling of the Piniada Valley has two major sources: one is associated with the fluvial dynamics of the Pinios River draining a wide area in Central Greece (Fig. 1), the other has a more local provenance with clastic materials produced from the reliefs directly surrounding the investigated valley (Fig. 2). The former type

of sediments commonly consist of fine-grained clastics and clay transported as bed load and suspended load, respectively, and mainly accumulated in the plain by the repeated flooding events. Diffuse marsh conditions associated with topographic lows and abandoned meanders are also common. The other major sedimentary source contributing to the infilling of the Piniada Valley was represented by the clastic deposits basically eroded from the rocky slopes of the several lateral valleys bordering the intermountain alluvial plain (Fig. 2). In this regard, it is noteworthy that the source areas of these ejection cones are largely represented by Triassic recrystallized limestone. Only locally, Palaeozoic schists and gneiss of the Pelagonian Zone and Pliocene fluvio-lacustrine deposits of the Central Hills dominate some of the hydrographic basins feeding the lateral ejection cones, west of Zarko and south of Koutsochero villages, respectively (Fig. 2; Caputo 1990; IGME 1985, 1998). As a consequence, while the prevailing materials from the Palaeozoic and Pliocene source areas locally accumulated within the Piniada Valley are represented by medium-to-fine-grained sands or silt, the sedimentary contribution from the areas characterized by carbonate outcrops mainly consist of monolithic coarse-grained breccias and/or conglomerates.

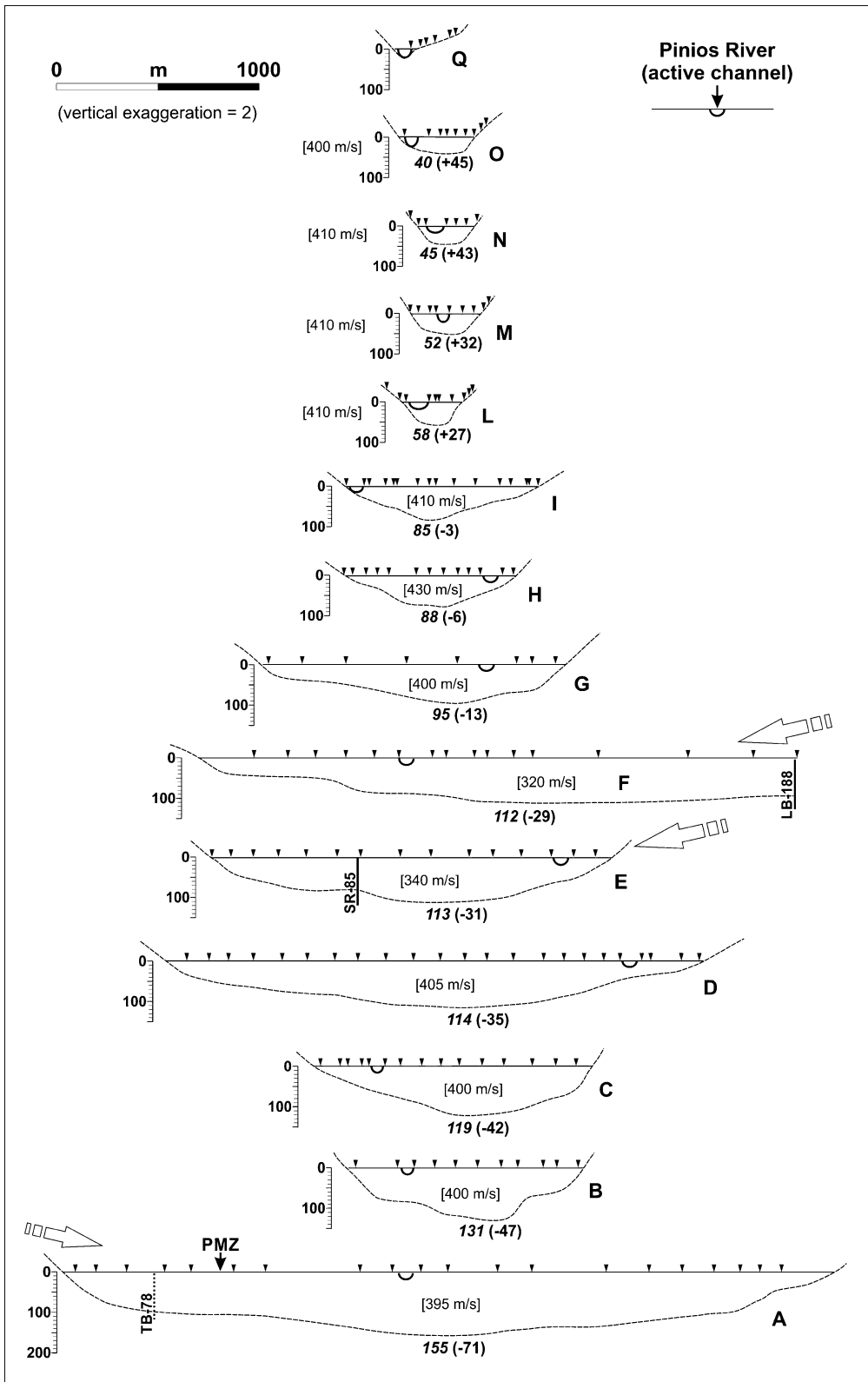
As above mentioned, it should be noted that in these geological conditions, even the chemistry of the drained waters was likely different. Indeed, the latter hydrographic basins were obviously much richer in carbonate solute and, as a further consequence, also the (incipient) diagenetic processes were laterally variable along the Piniada Valley infilling; cementation (mainly spatic calcite) was certainly more diffuse and intense in the cones of carbonate provenance and almost absent in the other ones. Also for this reason it is, therefore, reasonable to assume a slightly lower shear-wave velocity in correspondence of the lateral hydrographic basins that mainly drain the Palaeozoic schists–gneiss and the Pliocene clastics. On the other hand, this seismological inference obtained from the geological and stratigraphic constraints (i.e. sedimentary distribution) is in perfect agreement with the shear-wave velocity values calculated in correspondence of the available boreholes (Table 1). Fortified by these results and taking into account a reasonable

uncertainty of $\pm 10\%$, we attributed smoothly variable velocities (vertical average values) to the deposits infilling the Piniada Valley ranging between 320 and 440 m/s, which are typical values for loose-to-poorly consolidated alluvial deposits (e.g. Abu Zeid et al. 2014; Paolucci et al. 2015; Minarelli et al. 2016; Tarabusi and Caputo 2016). All these values are included in the Supplementary material.

4.3. Profiles Depth Conversion

Based on the above discussion, velocities and using the Herak et al. (2010) code, through a side-by-side stacks of the “converted” spectra along the profiles indicated in Fig. 3, we reconstructed pseudo-2D sections showing the geometry at depth of the bedrock top surface and the thickness of the Late Quaternary infilling. An example of this procedure is represented in Fig. 5c, which clearly shows that the bedrock depth progressively increases moving away from the external points of the profile, where indeed the bedrock is directly outcropping (i.e. no amplification), reaching a maximum value in a more or less central sector. Altogether, the deposits describe a lower concave upwards geometry topped by the flat topography.

It is worthy of note that the simplified procedure provided by the Herak et al. (2010) Matlab routine allows to use only a unique shear-wave velocity for the sedimentary layer overlying the bedrock thus implicitly assuming it is laterally and vertically uniform. Accordingly, for the depth conversion of each profile we reasonably assumed a mean value representative of the selected profile (indicated in Fig. 7). Whatsoever, the introduced simplification could not modify the overall geometry of the results. Indeed, all pseudo-2D sections crossing the Piniada Valley similarly document the presence of the bedrock at depth with basically the same pattern (Fig. 7) characterized by the deepening towards the central part of the section, that is to say a progressive shallowing towards the boundaries of the alluvial plain. Moreover, when observing all profiles in a perspective view following the path of the Piniada Valley (Fig. 7), an along river-flow progressive decrease of the maximum reconstructed depth to the bedrock is manifest. What is surprising, however, is



◀Figure 7

Pseudo-2D sections across the Piniada Valley showing the depth of the resonant surface (i.e. seismic bedrock) obtained by interpolation of several aligned HVSR analyses. Triangles indicate the projection of the measurement points along the transects. See Fig. 3 for traces location. Numbers in italics indicate the local depth from the field surface and in brackets the absolute altitude a.s.l.; all values are in metres. In square parentheses are indicated the shear-wave velocity used in each profile for the depth conversion. Approximately between the I and L sections occurs the progressive switch from a present-day flooding behaviour to a linear entrenching process by the Pinios River. PMZ indicates the location of the Plateia Magoula Zarkou archaeological site

the fact that the shallowing of the palaeovalley bottom and the associated thinning of the Late Quaternary deposits occur downstream relative to the modern Pinios River and not upstream, that is to say, from the Farkadona section towards the Kalamaki Gorge. We will further discuss this issue in the following section.

5. 3D Modelling

As anticipated above, the pseudo-2D sections represent an intermediate investigation step basically used for obtaining a preliminary picture of the palaeovalley geometry and for better planning the following field campaigns. Indeed, in a second working phase we carried out ca. 100 additional microtremor measurements along the Piniada Valley to investigate the sectors of the alluvial plain in between the several profiles and to refine the profiles themselves (Fig. 3). Sites were selected in the attempt of generating a regularly distributed grid of measurements. The single records were elaborated in the same way of the other sites along the transects, therefore, producing as many HVSR curves each characterized by its natural frequency.

Based on the distribution of the shear-wave velocities within the alluvial deposits infilling the Piniada Valley, as discussed in a previous section, we thus migrated all the additional measurements from the frequency domain to the depth domain, therefore, identifying the local depth of the seismic bedrock.

Finally, to reconstruct the 3D model of the palaeovalley underlying the recent alluvial deposits of the Pinios River, we thus interpolated on a GIS environment all depth values seismically obtained within the alluvial plain (i.e. inside the dashed line in

Fig. 3) together with the present-day digital elevation model outside of it. The ‘external’ DEM was used based on the assumption that, as a first approximation, the topography ‘outside’ the plain was not very different from the Late Pleistocene one. This strategy allows to give a major and more realistic geometric continuity to the buried valley slopes reconstructed on the basis of the less dense ‘internal’ seismic information. The results of this interpolation process are shown in Fig. 8. The present-day absolute altitude of the palaeovalley bottom varies between 40 and 45 m a.s.l., west of the Kalamaki Gorge, and ca. – 75 m (i.e. b.s.l.) near Farkadona.

As concerns the 1D assumption which is at the base of the applied geophysical method, we are aware that close to the borders of the alluvial plain, the buried flanks of the palaeovalley could have a slope with maximum dips of ca. 25°, though it is generally much less. The problem of the global valley resonance has been faced by several authors (Steimen et al. 2003; Frischknecht and Wagner 2004; Guiller et al. 2006; Roten et al. 2006; Guéguen et al. 2007) among which Bard and Bouchon (1985) recognize a critical ratio between the maximum valley depth and the width over which the sediment-thickness is at least half the maximum depth. According to the velocities used for the sedimentary cover in our investigated area, as obtained by calibration with the water wells (Table 1), and those attributed to the bedrock, the results of Bard and Bouchon (1985) clearly suggest that the Piniada Valley is far from being affected by 2D resonance effects and, therefore, we could safely apply the depth inversion according to Eq. (1). We also remind here that the major goal of this paper is to reconstruct the overall large-scale geometry of the entire Piniada Valley and not its morphological details.

6. Concluding Remarks

In this paper, we present the results of an extensive field campaign based on the systematic measurement of the seismic noise within the alluvial plain of the Piniada Valley (Fig. 2), which represent a major morphological anomaly along the hydrographic network of the Pinios River, the longest water

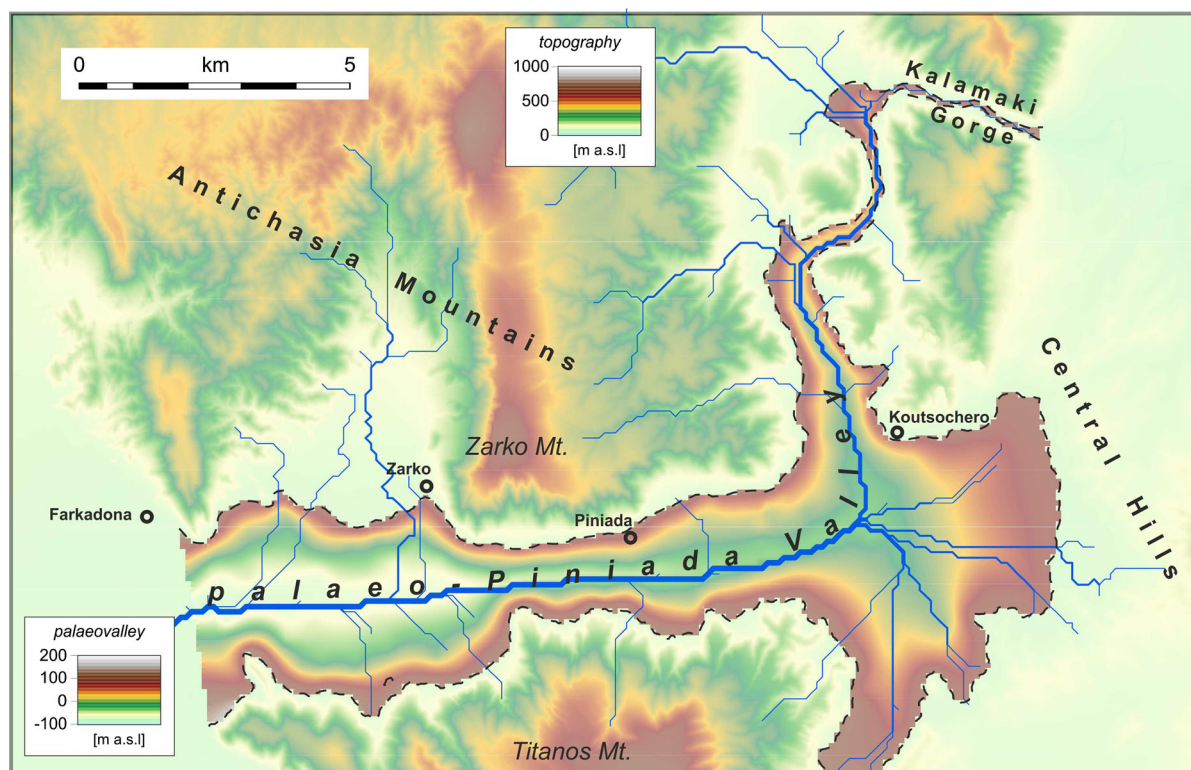


Figure 8

Digital elevation model of the investigated area showing the present-day topography and the interpolated palaeovalley bottom underlying the Late Quaternary infilling. Note the two different colour-coded scales for the areas, respectively, outside and inside the dashed line bordering the alluvial plain of the Piniada Valley. It is noteworthy that the recently buried south- and westwards palaeo-gradient was in the opposite direction with respect to the active Pinios River (Fig. 1). The likely palaeo-hydrographic network as automatically obtained using a conventional GIS tool (SAGA software) is also represented as a blue line

course in Greece (Fig. 1). To shed some light on this geographic and geological issue, the so-called local microtremor was recorded with a triaxial seismometer at more than 300 sites (Fig. 3). By applying the procedure proposed by Nakamura (1989), it was thus possible to obtain as many HVSr curves, most of them showing a well-marked peak varying between 20 and 0.6 Hz.

Moreover, based on the careful analysis of the available stratigraphic logs from boreholes drilled for irrigation purposes (Table 1) and performing dedicated measurements for their seismic noise calibration, the shear-wave velocities characterizing the infilling sediments overlying the bedrock have been attained ranging between 320 and 430 m/s, which are typical values for loose-to-poorly consolidated alluvial deposits (e.g. Abu Zeid et al. 2014;

Paolucci et al. 2015; Minarelli et al. 2016; Tarabusi and Caputo 2016). Based on these calibrations and geological–stratigraphical constraints, it was consequently possible to convert each HVSr curve from the frequency domain to the depth domain (Fig. 4) and, therefore, to obtain the depth to the (seismic) bedrock from the ground surface. In this regard, we should stress that a $\pm 10\%$ uncertainty in shear-wave velocity attributed to each site obviously implies a difference in the calculated depth to the bedrock at single measurement sites. However, the overall geometry of the reconstructed valley bottom could be not significantly affected by such uncertainties. In particular, no velocity uncertainty could justify the depth differences observed between, for example, transect A and transect O in Fig. 7, or across any of the shown profiles moving from the valley edge

towards the alluvial plain center in both directions. Accordingly, the overall geophysical results and the geological inferences should be considered well constrained.

Finally, working in a GIS environment and using both the present-day altitude of the measured sites and the corresponding obtained depths of the bedrock underlying the alluvial infilling, it was possible to interpolate all values for reconstructing a fully georeferenced 3D model of the palaeovalley bottom (Fig. 8). This model clearly shows that the palaeotopographic gradient of the Piniada Valley was directed south- and westwards (north and west of Koutsochero, respectively), that is to say in the opposite direction of the present-day river. In other words, during (Late?) Pleistocene the local hydrographic drainage was certainly flowing towards the present-day Karditsa Plain. Indeed, based on this combined digital elevation model and using another GIS tool included in the SAGA software, we also automatically reconstructed the hydrographic network that likely characterized the palaeovalley and its flanks sometimes during Late Pleistocene. This tentative drainage is also represented in Fig. 8.

In terms of palaeogeographic and tectonic evolution of this sector of Central Greece, the obtained results are remarkable because they clearly document for the first time that the two major Thessalian basins (Karditsa to the west and Larissa to the east) were not hydrographically connected till recently. On the other hand, the occurrence of very thick clay and turf sedimentary successions drilled in the Karditsa area (Kallergis et al. 1973), even few kilometres west and southwest of Farkadona and just few metres below the alluvial deposits associated with the modern Pinios River document the presence of a well-established lacustrine-marsh environment, the so-called Karditsa Lake, before the creation of the subaerial sedimentary conditions that we observe today. Remnants of this palaeo-environment in the form of widespread swamp areas in the central and eastern parts of the Karditsa Plain could be observed up to mid-twentieth century when the last major artificial draining and irrigation works modified the hydrography and morphology of the region. A similarly complex environmental and palaeogeographic evolution has been also reported for the Larissa area during Holocene times (Caputo et al.

1994). Similarly, sometimes during the (Late?) Quaternary the Piniada Valley was first abandoned by the major water course, as clearly documented by the geophysical results. As a working hypothesis, this was possibly due to a tectonically induced upstream capture as a consequence of the Late Pleistocene tectonic paroxysm associated with the activity of the nearby Larissa and Tyrnavos faults (Caputo and Pavlides 1993; Caputo 1993; Caputo et al. 1994, 2003). The valley was then progressively and rapidly infilled by the materials coming from the ‘western’ rivers and representing the major geophysical focus of the present research. As a consequence, the topographic (and hence hydraulic) gradient along the Piniada Valley was inexorably reversed, thus generating the definite connection between the western and the eastern plains we observe today.

Although more precise chronological data would be important for better constraining the above-described evolution, the final stages of these radical and dramatic hydrographic and geographic changes probably occurred after the last glacial maximum and mainly during the Holocene. It is thus very likely that the highly variable environmental conditions induced by these natural events persisted till recently and strongly influenced also the Neolithic settlements distribution within the Piniada Valley (Caputo et al., in prep.).

Acknowledgements

The present research was carried out in the frame of the Plateia Magoula Zarkou Project (resp. Eva Alam, Österreichische Akademie der Wissenschaften), which also financed the geological and geophysical campaigns. We thank the Editor (C. Braitenberg), an anonymous reviewer and I. Koukouvelas for their comments that helped improve a previous version of the manuscript.

REFERENCES

- Abu Zeid, N., Bignardi, S., Caputo, R., Mantovani, A., Tarabusi, G., & Santarato, G. (2014). Shear-wave velocity profiles across the Ferrara Arc: A contribution for assessing the recent activity of blind tectonic structures. 33^o Convegno Nazionale GNGTS, Bologna, November 25–27 2014, *Atti, 1*, 117–122, ISBN 978-88-940442-1-8.
- Aki, K., & Richards, P. (2002). *Quantitative seismology* (2nd ed.). Sausalito: University science books.

- Albarelo, D., Cesi, C., Eulilli, V., Guerrini, F., Lunedei, E., Paolucci, E., et al. (2011). The contribution of the ambient vibration prospecting in seismic microzonation: an example from the area damaged by the 26th April 2009 l'Aquila (Italy) earthquake. *Bollettino di Geofisica Teorica ed Applicata*, 52(3), 513–538. <https://doi.org/10.4430/bgta0013>.
- Asten, M. W. (1978). Geological control of the three-component spectra of Rayleigh-wave microseisms. *Bulletin of the Seismological Society of America*, 68(6), 1623–1636.
- Asten, M. W., & Henstridge, J. D. (1984). Arrays estimators and the use of microseisms for reconnaissance of sedimentary basins. *Geophysics*, 49(11), 1828–1837.
- Bard, P. (1998). Microtremor measurements: A tool for site effect estimation?. In *Proc. Second Int. Symp. Effects of Surface Geology on Seismic Motion*, Vol. 3 (pp. 1251–1279).
- Bard, P.-Y., Bouchon, M. (1985). The two-dimensional resonance of sediment-filled valleys. *Bulletin of the Seismological Society of America*, 75(2), 519–541.
- Bard, P.-Y., Acerra, C., Alguacil, G., Anastasiadis, A., Atakan, K., Azzara, R., et al. (2005). Guidelines for the implementation of the H/V spectral ratio technique on ambient vibrations measurements, processing and interpretation. Deliverable D23.12 of the SESAME project, April 2005. <http://www.SESAME-FP5.obs.ujf-grenoble.fr>.
- Ben-Menahem, A., & Singh, S. (1981). *Seismic waves and sources*. New York: Springer.
- Bignardi, S., Mantovani, A., & Abu, Zeid N. (2016). OpenHVSr: Imaging the subsurface 2D/3D elastic properties through multiple HVSR modeling and inversion. *Computers & Geosciences*, 93, 103–113.
- Bourbié, T., Coussy, O., & Zinszner, B. (1987). *Acoustics of porous media* (p. 334). Houston: Gulf Publishing Company.
- Caputo, R. (1990). *Geological and structural study of the recent and active brittle deformation of the Neogene-Quaternary basins of Thessaly (Central Greece)*. Scientific Annals, Aristotle University of Thessaloniki., 5 encl., 2 vol., Thessaloniki.
- Caputo, R. (1993). Morphotectonics and kinematics along the Timavos Fault, northern Larissa Plain, mainland Greece. *Zeits. für Geomorph. N.F. Suppl.-Bd.* 94, 167–185.
- Caputo, R., Bravard, J.-P., & Helly, B. (1994). The Pliocene-Quaternary tecto-sedimentary evolution of the Larissa Plain (Eastern Thessaly, Greece). *Geodinamica Acta*, 7, 57–85.
- Caputo, R., & Pavlides, S. (1993). Late Cainozoic geodynamic evolution of Thessaly and surroundings (central-northern Greece). *Tectonophysics*, 223(3–4), 339–362.
- Caputo, R., Piscitelli, S., Oliveto, A., Rizzo, E., & Lapenna, V. (2003). The use of electrical resistivity tomography in active tectonics. Examples from the Tyrnavos Basin, Greece. *Journal of Geodynamics*, 36(1–2), 19–35.
- Castellaro, S., & Mulargia, F. (2009). Vs30 estimates using constrained H/V measurements. *Bulletin of the Seismological Society of America*, 99, 761–773.
- Castellaro, S., Mulargia, F., & Bianconi, L. (2005). Passive seismic stratigraphy: a new efficient, fast and economic technique. *Journal Geotechnical Environment Geological*, 3, 51–77.
- Chatelain, J. L., & Guillier, B. (2013). Reliable fundamental frequencies of soils and buildings down to 0.1 Hz obtained from ambient vibration recordings with a 4.5-Hz sensor. *Seismological Research Letters*, 84, 199–209.
- D'Amico, V., Picozzi, M., Baliva, F., & Albarello, D. (2008). Ambient noise measurements for preliminary site-effects characterization in the urban area of Florence. *Bulletin of the Seismological Society of America*, 98, 1373–1388. <https://doi.org/10.1785/0120070231>.
- Doutsos, T., Pe-Piper, G., Boronkay, K., & Koukouvelas, I. (1993). Kinematics of the central Hellenides. *Tectonics*, 12(4), 936–953.
- Fäh, D., Kind, F., & Giardini, D. (2001). A theoretical investigation of average H/V ratios. *Geophysical Journal International*, 145, 535–549.
- Frischknecht, C., & Wagner, J. J. (2004). Seismic soil effect in an embanked deep Alpine valley: A numerical investigation of two-dimensional resonance. *Bulletin of the Seismological Society of America*, 94(1), 171–186. <https://doi.org/10.1785/0120020158>.
- Gallipoli, M. R., Mucciarelli, M., Gallicchio, S., Tropeano, M., & Lizza, C. (2004). Horizontal to Vertical Spectral Ratio (HVSR) measurements in the area damaged by the 2002 Molise, Italy, earthquake. *Earthquake Spectra*, 20(S1), S81–S93. <https://doi.org/10.1193/1.1766306>.
- Gomberg, J., Waldron, B., Schweig, E., Hwang, H., Webbers, A., VanArsdale, R., et al. (2003). Lithology and shear-wave velocity in Memphis, Tennessee. *Bulletin of the Seismological Society of America*, 93(3), 986–997.
- Gosar, A., & Lenart, A. (2010). Mapping the thickness of sediments in the Ljubljana Moor basin (Slovenia) using microtremors. *Bulletin of Earthquake Engineering*, 8, 501–518. <https://doi.org/10.1007/s10518-009-9115-8>.
- Guéguen, P., Cornou, C., Garambois, S., & Banton, J. (2007). On the limitation of the H/V spectral ratio using seismic noise as an exploration tool: Application to the Grenoble valley (France), a small apex ratio basin. *Pure and Applied Geophysics*, 164(1), 115–134. <https://doi.org/10.1007/s00024-006-0151-x>.
- Guiller, B., Cornou, C., Kristek, J., Moczo, P., Bonnefoy-Claudet, S., Bard, P.-Y., et al. (2006). Simulation of seismic ambient vibrations: does the H/V provide quantitative information in 2D-3D structures? In *Third Int. Symp. Effects of Surface Geology on Seismic Motion, Grenoble, 30 August–1 September 2006, Proceedings*, Paper Number 185.
- Gutenberg, B. (1958). Microseisms. *Advances in Geophysics*, 5, 53–92.
- Herak, M. (2008). ModelHVSR—A Matlab tool to model horizontal-to-vertical spectral ratio of ambient noise. *Computers & Geosciences*, 34, 1514–1526.
- Herak, M., Allegretti, I., Herak, D., Kuk, K., Kuk, V., Marić, K., et al. (2010). HVSR of ambient noise in Ston (Croatia): Comparison with theoretical spectra and with the damage distribution after the 1996 Ston-Slano earthquake. *Bulletin of Earthquake Engineering*, 8, 483–499.
- Hinzen, K. G., Scherbaum, F., & Weber, B. (2004). On the resolution of H/V measurements to determine sediment thickness, a case study across a normal fault in the Lower Rhine embayment, Germany. *Journal of Earthquake Engineering*, 8, 909–926.
- Ibs-von, Seht M., & Wohlenberg, J. (1999). Microtremor measurements used to map thickness of soft sediments. *Bulletin of the Seismological Society of America*, 89, 250–259.
- IGME (Institute of Geology and Mineral Exploration). (1985). *Geological map of Greece 1:50.000, Sheet Larissa*. Athens.
- IGME (Institute of Geology and Mineral Exploration). (1998). *Geological map of Greece 1:50.000, Sheet Farkadona*. Athens.
- Kallergis, G., Morfis, A., Papaspyropoulos, Ch., & Christodoulou, Th. (1973). Hydrogeological investigation in Western Thessaly. *Hrydrol. Hydrogeol. Invest., I.G.M.E.*, 8, 1–126 (Athens).
- Kawase, H., Matsushima, S., Satoh, T., & Sánchez-Sesma, F. J. (2015). Applicability of theoretical horizontal-to-vertical ratio of microtremors based on the diffuse field concept to previously

- observed data. *Bulletin of the Seismological Society of America*, 105(6), 3092–3103. <https://doi.org/10.1785/0120150134>.
- Koller, M., Chatelain, J.-L., Guillier, B., Duval, A.-M., Atakan, K., Bard, P.-Y. et al. (2004). Practical user guidelines and software for the implementation of the H/V ratio technique: measuring conditions, processing method and results interpretation. In *13th World Conf. Earthq. Eng., Vancouver, August 2004, Proceedings*, paper # 3132.
- Lachet, C., & Bard, P.-Y. (1994). Numerical and theoretical investigations on the possibilities and limitations of Nakamura's technique. *Journal of Physics of the Earth*, 42, 377–397.
- Lermo, J., & Chavez-Garcia, F. J. (1993). Site effect evaluation using spectral ratios with only one station. *Bulletin of the Seismological Society of America*, 83, 1574–1594.
- Lermo, J., & Chavez-Garcia, F. J. (1994). Are microtremors useful in site response evaluation? *Bulletin of the Seismological Society of America*, 84, 1350–1364.
- Lontsi, A. M., Sánchez-Sesma, F. J., Molina-Villegas, J. C., Ohrnberger, M., & Krüger, F. (2015). Full microtremor H/V(z; f) inversion for shallow subsurface characterization. *Geophysical Journal International*, 202, 298–312.
- Lunedei, E., & Albarello, D. (2010). Theoretical HVSR curves from full wavefield modelling of ambient vibrations in a weakly dissipative layered earth. *Geophysical Journal International*, 181, 1093–1108.
- Lunedei, E., & Albarello, D. (2015). HVSR curve by a full-wavefield model of ambient vibrations generated by a distribution of correlated surface sources. *Geophysical Journal International*, 201, 1140–1153.
- Mantovani, A. (2016). Recent tectonic activity of the central sector of the Ferrara Arc emphasized by a multidisciplinary approach. Ph.D. thesis University of Ferrara, pp. 250.
- Matsushima, S., Hirokawa, T., De Martin, F., Kawase, H., & Sánchez-Sesma, F. J. (2014). The effect of lateral heterogeneity on horizontal-to-vertical spectral ratio of microtremors inferred from observation and synthetics. *Bulletin of the Seismological Society of America*, 104(1), 381–393. <https://doi.org/10.1785/0120120321>.
- Migiros, G., Bathrellos, G. D., Skilodimou, H. D., & Karamousalis, T. (2011). Piniós (Peneus) River (Central Greece): Hydrological-geomorphological elements and changes during the quaternary. *Central European Journal of Geosciences*, 1(2), 215–228. <https://doi.org/10.2478/s13533-011-0019-1>.
- Minarelli, L., Amoroso, S., Tarabusi, G., Stefani, M., & Pulelli, G. (2016). Down-hole geophysical characterization of middle-upper quaternary sequences in the Apennine Foredeep, Mirabello, Italy. *Annals of Geophysics*, 59(5), S0543. <https://doi.org/10.4401/ag-7114>.
- Mucciarelli, M., & Gallipoli, M. R. (2001). A critical review of 10 years of microtremor HVSR technique. *Bollettino di Geofisica Teorica ed Applicata*, 42, 255–266.
- Mulargia, F., & Castellaro, S. (2016). HVSR deep mapping tested down to ~ 1.8 km in Po Plane Valley, Italy. *Physics of the Earth and Planetary Interiors*, 261, 17–23.
- Mundepi, A. K., & Mahajan, A. K. (2010). Site response evolution and sediment mapping using horizontal to vertical spectral ratios (HVSR) of ground ambient noise in Jammu City, NW India. *Journal of the Geological Society of India*, 75, 799–806.
- Nakamura, Y. (1989). A method for dynamic characteristics estimation of subsurface using microtremor on the ground surface. *Quarterly Reports Railway Technical Research Institute (RTRI)*, 30, 25–33.
- Nakamura, Y. (2000). Clear identification of fundamental idea of Nakamura's technique and its applications. In *Proceedings of the Twelfth World Conference on Earthquake Engineering*. New Zealand.
- Ohrnberger, M., Scherbaum, F., Krüger, F., Pelzing, R., & Reamer, S. K. (2004). How good are shear wave velocity models obtained from inversion of ambient vibrations in the Lower Rhine Embayment (N.W. Germany)? *Bollettino di Geofisica Teorica ed Applicata*, 45, 215–232.
- Oliveto, A. N., Mucciarelli, M., & Caputo, R. (2004). HVSR prospections in multi-layered environments: An example from the Tyrnavos Basin (Greece). *J. Seismol.*, 8, 395–406.
- Paolucci, E., Albarello, D., D'Amico, S., Lunedei, E., Martelli, L., Mucciarelli, M., et al. (2015). A large scale ambient vibration survey in the area damaged by May–June 2012 seismic sequence in Emilia Romagna, Italy. *Bulletin of Earthquake Engineering*, 13(11), 3187–3206.
- Parker, E. H., Jr., & Hawman, R. B. (2012). Multichannel Analysis of Surface Waves (MASW) in Karst Terrain, Southwest Georgia: Implications for Detecting Anomalous Features and Fracture Zones. *Journal of Environmental and Engineering Geophysics*, 17(3), 129–150.
- Parolai, S., Bormann, P., & Milkereit, C. (2001). Assessment of the natural frequency of the sedimentary cover in the Cologne area (Germany) using noise measurements. *Journal of Earthquake Engineering*, 5, 541–564.
- Roten, D., Fäh, D., Cornou, C., & Giardini, D. (2006). 2D resonances in Alpine valleys identified from ambient vibration wavefields. *Geophysical Journal International*, 165, 889–905. <https://doi.org/10.1111/j.1365-246X.2006.02935.x>.
- Sánchez-Sesma, F. J., Rodríguez, M., Iturrarán-Viveros, U., Luzón, F., Campillo, M., Margerin, L., et al. (2011). A theory for microtremor H/V spectral ratio: Application for a layered medium. *Geophysical Journal International*, 186(1), 221–225.
- Scherbaum, F., Hinzen, K.-G., & Ohrnberger, M. (2003). Determination of shallow shear wave velocity profiles in the Cologne/Germany are using ambient vibrations. *Geophysical Journal International*, 152, 597–612.
- SESAME European project. (2005). Guidelines for the implementation of the H/V spectral ratio technique on ambient vibrations—Measurements, processing and interpretation. Deliverable D23.12. http://sesame-fp5.obs.ujf-grenoble.fr/SES_TechnicalDoc.htm.
- Steimen, S., Fäh, D., Kind, F., Schmid, C., & Giardini, D. (2003). Identifying 2D resonance in microtremor wave fields. *Bulletin of the Seismological Society of America*, 93(2), 583–599. <https://doi.org/10.1785/0120000264>.
- Tarabusi, G., & Caputo, R. (2016). The use of HVSR measurements for investigating buried tectonic structures: The Mirandola anticline, northern Italy, as a case study. *International Journal of Earth Sciences*, 106, 341–353. <https://doi.org/10.1007/s00531-016-1322-3>.
- Tsai, N., & Housner, G. (1970). Calculation of surface motions of a layered half-space. *Bulletin of the Seismological Society of America*, 60, 1625–1651.